Journal of Ultrafine Grained and Nanostructured Materials
https://jufgnsm.ut.ac.ir
Vol. 54, No.1, June 2021, pp. 58-63
Print ISSN: 2423-6845 Online ISSN: 2423-6837
DOI: 10.22059/jufgnsm.2021.01.06

Synthesis and antibacterial performance of Ag/Co_2O_3/graphitic carbon nitride

Mahdieh Chegeni*, Mozhgan Mehri, Zahra Shokri Rozbahani

Department of Chemistry, Faculty of Science, Ayatollah Boroujerdi University, Boroujerd, Iran.

Recieved: 24 September 2020; Accepted: 17 December 2020
** Corresponding author email: mahdieh.chegeni@abru.ac.ir*

ABSTRACT

The $Ag/Co_2O_3/g\text{-}C_3N_4$ as a novel nanocomposite was synthesized using a facile strategy by "one pot" method. The as-prepared nanocomposite was applied to improve the antibacterial effect against *Escherichia coli* and *Staphylococcus aureus* bacteria. The nanocomposite was characterized by Fourier transform infrared spectroscopy, X-ray Diffraction, and Scanning Electron Microscopy techniques. The strong interaction beetween the plans of graphitic carbon nitride ($g\text{-}C_3N_4$) and other particles can be resulted to stable nanocomposite. The zone inhibition of nanocomposite was determined for Gram-positive and Gram-negative bacteria. The findings showed the better activity of as-prepared nanocomposite against Gram negative bacteria rather to Gram positive bacteria. The $Ag/Co_2O_3/g\text{-}C_3N_4$ was shown good antibacterial effect compared to $g\text{-}C_3N_4$ and Ag patricles. Further, Colony Forming Unit was indicated the antibacterial behavior of as-prepared composite. The present study can explain insight into the synthesis of heterojunction composite for disinfection.

Keywords: *Biomaterials, nanoparticles, graphitic carbon nitride, antibacterial activity*.

1. Introduction

Nowadays, the improvement of human health is a main subject throughout the world. In this regard, one of the most important challenges would be bacterial infections. The pathogenic microorganisms are extensively dispersed in our everyday life environments including water, dust, door, toilet, lab, etc [1]. To address this problem, the application of antibiotics is a common method. However, there are several disadvantages including water pollutants, the need for high amounts of drug, and increasing antibiotic resistance. *Escherichia coli* (*E. coli*, Gram-negative) and Staphylococcus aureus (*S. aureus*, Gram-positive) are well-known pathogenic bacteria, which can be harmful to human health, causing infectious diseases [2].

In the past few years, different materials have been used against bacterial activities; among which, carbon-based compounds have exhibited effective results on bacterial diseases. In recent years, graphitic carbon nitride ($g\text{-}C_3N_4$) introduced as a nitrogen-rich polymer with applications as a semiconductor, adsorbent, and photocatalyst [3,4]. Among synthesis methods of $g\text{-}C_3N_4$, the thermal polycondensation were reported as an efficient strategy, due to its simplicity and low cost. Several methods can be applied for modification of the bulk $g\text{-}C_3N_4$ properties such as nanostructure formation, surface engineering, and heterostructure construction [5]. According to previous literatures, the adsorption properties and photocatalyst performance of $g\text{-}C_3N_4$ were modified

by the synthesis of g-C_3N_4-based heterostructure composite [5]. Construction of g-C_3N_4-based heterostructures by metal nanoparticles (NPs) can be applied as a suitable method to improve g-C_3N_4 applications [6]. When an efficient semiconductor is placed in contact with bulk g-C_3N_4, the spatial separation of photogenerated electron–hole pairs can be increased [7]. To improve the photocatalytic activity of g-C_3N_4, the Z-scheme systems were proposed. In this system, charge transfer between two semiconductors can be accrued by the injection of the photo-generated electrons in the conduction band, valance band, and the hole of g-C_3N_4 [8]. On the other hand, g-C_3N_4-based multicomponent composite can exhibit improved properties.

The presence of some metals such as phosphorus [9], sulphur [10], Zinc [11], and silver [12] can modify particular features of g-C_3N_4-based heterostructure compound. Cobalt oxide (Co_2O_3) possesses unique properties including catalytic activity, catalyzing oxygen evolution reaction (OER), stability, and p-type semiconductivity [13].

Further, Ag nanoparticles are considered as one of the important biocide agents, exhibiting a vast range of antibacterial applications [14]. In recent years, different types of composites were reported such as MoS_2 nanosheets loaded with Ag NPs [14], sulfur-doped carbon quantum dots (S-CQDs)/hollow tubular g-C_3N_4 [15], and Ag-ZnO/g-C_3N_4 [16]. However, some of these compounds have shown drawbacks, which limit their extensive applications, such as complicated preparation procedure, high cost, and instability. For these reasons, designing and development of new composites would be required. In the present research, a novel composite was afforded to improve the biocompatibility of g-C_3N_4 through the synthesis of heterostructure composite, which can enhance the antibacterial properties of the bulk g-C_3N_4. Ag NPs and cobalt oxide are capable of enhancing the antibacterial and photocatalytic activities of Ag/Co_2O_3/g-C_3N_4 nanocomposite. The as-prepared nanocomposite can be introduced as an appropriate candidate for water purification applications.

2. Experimental

2.1. Material and methods

Melamine, sulfuric acid (H_2SO_4), nitric acid (HNO_3), cobalt nitrate ($Co(NO_3)_3$), and silver nitrate ($AgNO_3$) were purchased from Merck Company (Darmstadt, Germany), and all the chemicals were used as received.

2.2. Preparation of g-C_3N_4

The direct pyrolysis of melamine was employed to obtain bulk g-C_3N_4. The yellow powder was prepared by placing 5 g of melamine in alumina crucible, followed by heating at 580 °C for 2 h [17].

2.3. Synthesis of Ag/Co_2O_3/g-C_3N_4

First, 0.5 g of $Co(NO_3)_3$ was added to distilled water (50 mL), then g-C_3N_4 was slowly dropped into the $Co(NO_3)_3$ solution, and this mixture was filtrated and dried at 80 °C. The solution was stirred for 30 min, and 0.2 g $AgNO_3$ was added to the mixture. The ultraviolet light (300 W Xe lamp, 345 nm cut-off filter) was used to reduce Ag^+ to Ag nanoparticles. The value of Ag^+ were determined 41.67 ppm by Inductively Coupled Plasma (ICP). This synthesis strategy was studied using different mass ratios of the components (1:3 and 1:4 of $Co(NO_3)_3$:g-C_3N_4) to obtain the best results.

2.4. Antimicrobial activity

The agar cup-plate method was employed to evaluate the antibacterial activity of Ag/Co_2O_3/g-C_3N_4. This method was performed according to CLSI standards [18]. Typically, plates containing Müller-Hinton agar medium were prepared by wells with a 0.6 mm diameter, then 0.1 µl of bacterial suspensions with turbidity equivalent to half McFarland were cultured under same conditions. 10.0 µl of nanocomposite (0.300 µg per well plate) was poured into the wells, the plates were incubated at 37° C for 24 h. The antimicrobial activity was determined for each microorganism by measuring the growth inhibition zone.

Micro-well dilution assay method was applied to evaluate minimum inhibitory concentration (MIC) [19]. The 96-well plates were prepared by dispensing well in 95 ml of H_2O. The 5 µl bacterial suspension, 0.5 dilution McFarland, and 100 µl nanocomposite were added to each plate, and the plate was heated in an incubator at 37 ° C for 24 h.

Antibacterial activity of Ag/Co_2O_3/g-C_3N_4 nanocomposite was investigated by colony forming unit (CFU) reduction assay [20]. Microorganisms (104-105 CFU/ml of *E. coli* or *S. aureus*) were grown in flasks containing 10 ml of tryptic soy agar (TSB) at 37 °C for 5 h. The 25 mg of nanocomposite was dispersed in 25 ml of TSB at 37 °C under UV light. The suspension was taken out test tube after contact times (30, 60, 90, and 120 min). The diluted solution was inoculated on nutrient agar plates and incubated at 37 °C for 24 h. The count of bacterial

colonies was counted on each plate. A similar procedure was performed without $Ag/Co_2O_3/g-C_3N_4$ nanocomposite as a control assay.

2.5. Characterization

The Ag/Co_2O_3/S-doped graphitic carbon nitride was characterized by various techniques including Fourier transform infrared spectroscopy (FT-IR, Unicam-Galaxy 5000 with KBr pellets), X-ray Diffraction (XRD, Panalytical Xpertpro diffractometer using Cu Kα radiation, λ= 1.54178 Å), and Field Emission Scanning Electron Microscopy (FESEM, Tescan Mira3-Lmu). Inductively coupled plasma (ICP) was performed by Spectro Arcos, Germany.

3. Results and discussion

The different mass ratios of precursor were studied, and the 1:4 ratio of $Co(NO_3)_3$:g-C_3N_4 was shown the best result.

FT-IR spectra of the g-C_3N_4 and $Ag/Co_2O_3/g-C_3N_4$ are seen in Fig. 1. In the spectrum of g-C_3N_4, the peak at 808.58 cm^{-1} is shown, that belongs to the *s*-triazine ring [21]. The same peak at 808.52 cm^{-1} locates in the $Ag/Co_2O_3/g-C_3N_4$ composite. In both of spectrum, the aromatic C=N stretching frequency is observed at around 1220 and 1650 cm^{-1}. The absorption peak at 3160 cm^{-1} is resulted from stretching mode of -OH group in the spectrum of g-C_3N_4, but this peak in the as-prepared compared is board, due to interaction between the components of composite. The peaks at 550-650 cm^{-1} are related to metal-oxygen bonds such as the Co-O stretching frequency.

The XRD pattern was employed to obtain the structures of the samples. As illustrated in Fig. 2,

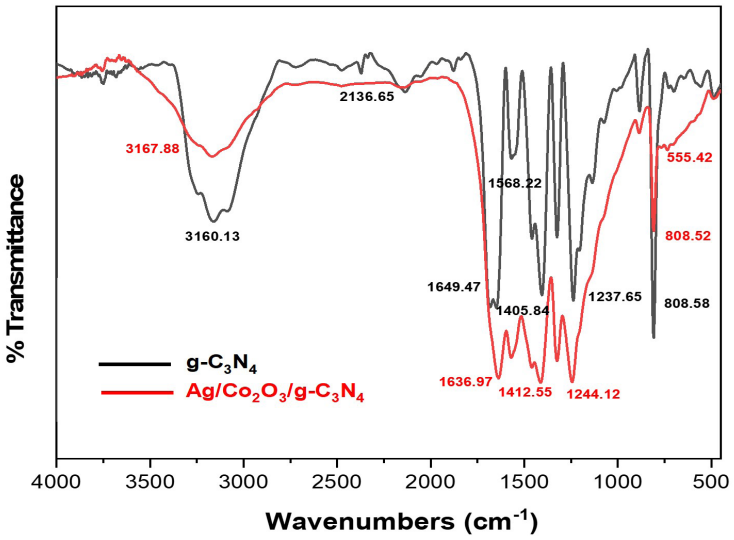

Fig. 1- FT-IR spectra of g-C_3N_4 and $Ag/Co_2O_3/g-C_3N_4$ composite.

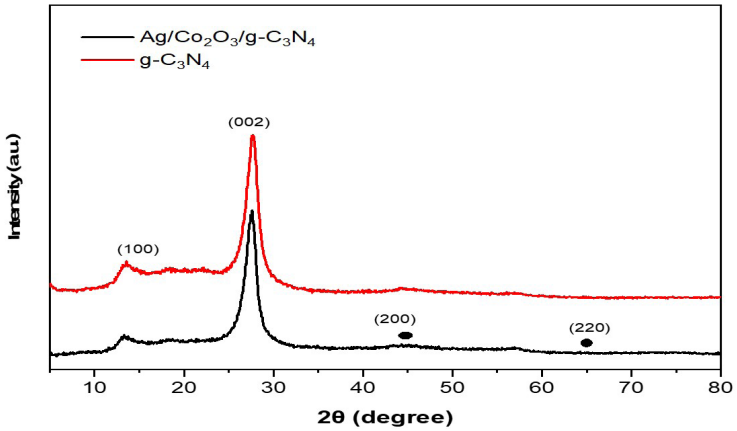

Fig. 2- XRD spectra of g-C_3N_4 and $Ag/Co_2O_3/g-C_3N_4$ composite.

the main peaks of g-C_3N_4 and Ag/Co_2O_3/g-C_3N_4 XRD patterns are similar together. In the XRD pattern of g-C_3N_4, the aromatic system can be assigned by peaks at 27.6° (0 0 2) and 13.3° (1 0 0), which are corresponded to hexagonal graphitic aromatic system (JCPDS: 87–1526). Further, these peaks are seen in the XRD pattern of Ag/Co_2O_3/g-C_3N_4 [21,22]. As shown in the XRD pattern of as-prepared composite, the major peaks are appeared at 38.7°, 44.7°, 63.01°, relevant to (1 1 1), (2 0 0), and (2 2 0) of fcc phase. The structure of Ag/Co_2O_3/g-C_3N_4 can be confirmed by (JCPDS: 01-079-0035), and the high dispersion of Ag/Co_2O_3/g-C_3N_4 resulted to low diffraction peaks. Also, the size of the crystalline particles was approximately 28 nm.

Fig. 3 depicts the morphologies of g-C_3N_4 and Ag/Co_2O_3/g-C_3N_4 composite in FESEM images. The smooth and sheet structure of g-C_3N_4 can be observed in Fig. 3(a-b). These Figures show graphite-like and wrinkled structure. The agglomeration can becaused to multilayer structure. As illustrated in Fig. 3(c-d), the particles are visible on g-C_3N_4 sheets, due to the formation of based-g-C_3N_4 composite by Co and Ag interaction with C– N–, –C=N– bonds. The average size of Ag/Co_2O_3/g-C_3N_4 nanocomposite are seen between 9.58-35.05 nm.

The antibacterial activity of Ag/Co_2O_3/g-C_3N_4 composite was studied using *E. coli* (ATCC 10536) and *S. aurous* (ATCC 29737) bacteria. The agar diffusion method was employed to investigate antibacterial effects. The Table 1 demonstrates the information of inhibition zones. The clear area (ZOIs) obtained around the g-C_3N_4 showed negligible antibacterial properties (Figure 4(a,b)). The Ag/Co_2O_3/g-C_3N_4 nanocomposite was shown better antibacterial activity compered to pure g-C_3N_4. The small size of as-prepared nanocomposite can be increased antibacterial activity, due to loading Co and Ag in g-C_3N_4 by successful attachment. In addition, the metal oxide has a positive charge, and it can be attracted a negative charge of microorganism. Further, the attachment of components can be reduced recombination of electron-hole. According to the results, higher antibacterial effect of Ag/Co_2O_3/g-C_3N_4 was observed against *Staphylococcus aureus* compared to *Escherichia coli*, and *S. aureus*

Table 1- The information data of antibacterial activity of Ag/Co_2O_3/g-C_3N_4

Bacteria strains	Zone of inhibition (mm)		MIC (µg/ml)
	Ag/Co_2O_3/g-C_3N_4	Ag NPs	Ag/Co_2O_3/g-C_3N_4
Escherichia coli	14	13.8	125
Staphylococcus aureus	16	10.1	250

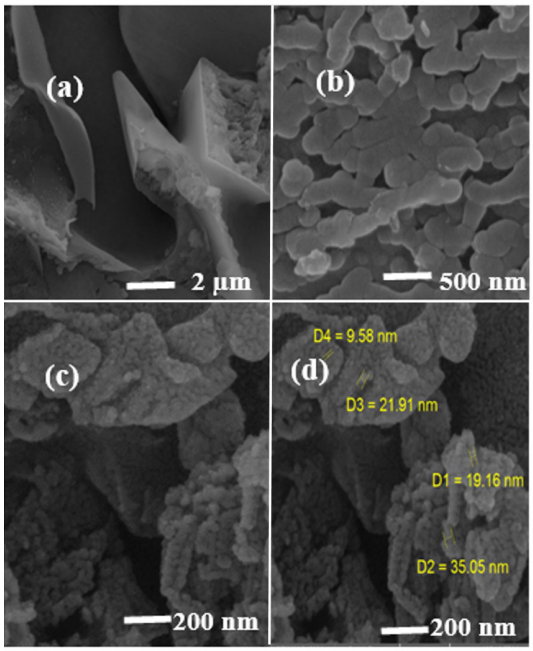

Fig. 3- FESEM images of g-C_3N_4 and Ag/Co_2O_3/g-C_3N_4.

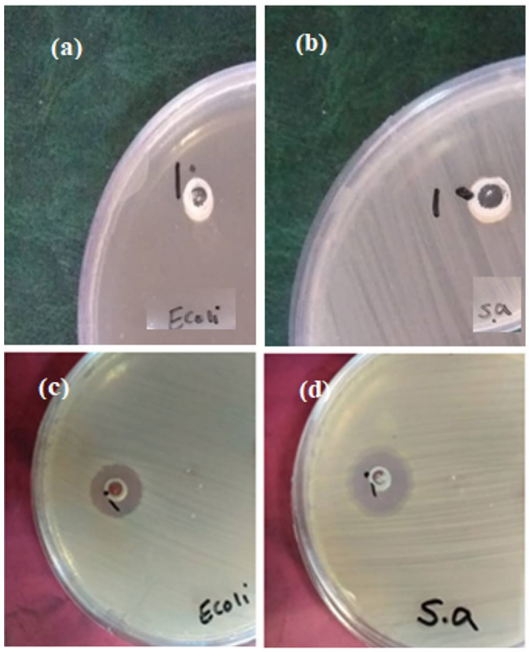

Fig. 4- Inhibition zones for *E. coli* and *S. aureus* (a,b) g-C_3N_4 (c,d) Ag/Co_2O_3/g-C_3N_4

bacteria could be killed at higher concentrations of the test compounds (Table 1). Minimum inhibitory concentration (MIC) and inhibition zone (Fig. 4) explain the antibacterial activity of $Ag/Co_2O_3/g\text{-}C_3N_4$ composite compared to Ag NPs. Results indicated that the $Ag/Co_2O_3/g\text{-}C_3N_4$ nanocomposite could prevent the bacterial activity, and loading of Ag NPs on $g\text{-}C_3N_4$ resulted in better performance of Ag NPs.

As shown in Fig. 5, SEM analyze is used to investigate the cellular morphological changes of *S. aureus* and *E. coli*. The *S. aureus* and *E. coli* bacteria have shown sphere shaped and rod-shaped morphologies with smooth surface before treatment [20,22]. After the antibacterial behavior of $Ag/Co_2O_3/g\text{-}C_3N_4$ nanocomposite, the cellular membrane of bacteria damaged and showed disruptions on cell well and resulted to cell death.

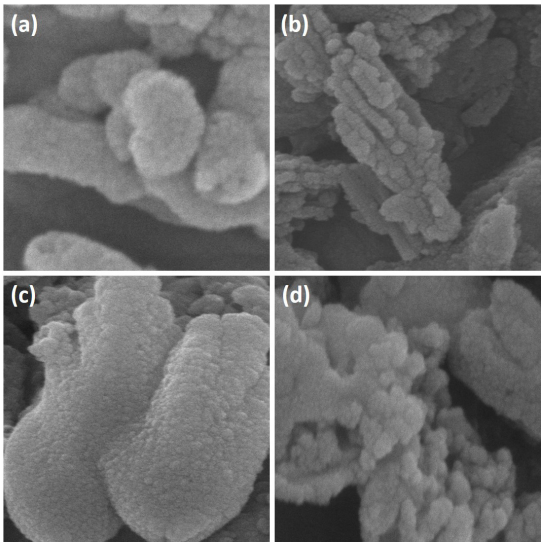

Fig. 5- SEM images of (a,b) *E. coli* and (c,d) *S. aureus* treated with $Ag/Co_2O_3/g\text{-}C_3N_4$ nanocomposite.

The antibacterial activity of $Ag/Co_2O_3/g\text{-}C_3N_4$ nanocomposite are shown in Fig. 6 (a,b). The results show that the concentration of both *E. coli* and *S. aureus* bacteria are decreased, and the growth rate of bacterial were reduced in the presence of nanocomposite after 120 min. Based on the results, the nanocomposite can be acted against bacteria. According to reactive oxygen species (ROS) mechanism, the nanocompoite was absorbed UV irradiation, and active species including e^-, h^+ ($O_2^{\cdot-}$), hydroxyl radical (OH^-), and hydrogen peroxide (H_2O_2) were generated [20-23]. Then the bacteria were killed by entering H_2O_2 into the cell wall, because of the cross-link reaction between the thymine bases and the strand of DNA. This findings can be explained the antibacterial activity of $Ag/Co_2O_3/g\text{-}C_3N_4$ nanocomposite against pathogen.

4. Conclusions

In the present study, $Ag/Co_2O_3/g\text{-}C_3N_4$ was synthesized via a simple method, and was subsequently characterized using Fourier transform infrared spectroscopy, X-ray diffraction, and field emission scanning electron microscopy. The antibacterial activity of $Ag/Co_2O_3/g\text{-}C_3N_4$ nanocomposite was demonstrated against Gram negative (*Escherichia coli*) and Gram-positive (*Staphylococcus aureus*) bacteria. The inhibition zones were obtained 14 and 16 mm against *E. coli* and *S. aureus* bacteria, respectively. According to CFU assay, the amounts of bacteria were decreased rather to control tests. The $Ag/Co_2O_3/g\text{-}C_3N_4$ can be used as a heterostructure composite for antibacterial activity and suitable choice for water purification.

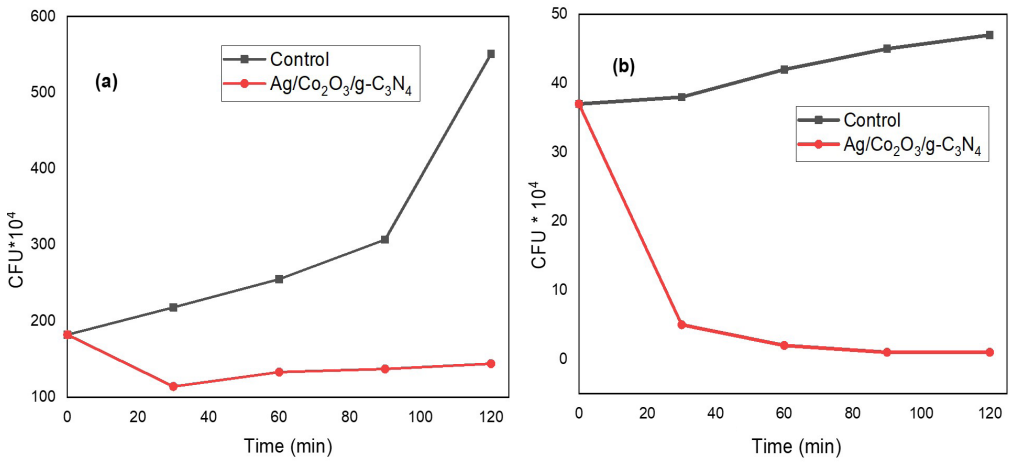

Fig. 6- CFU assay results of $Ag/Co_2O_3/g\text{-}C_3N_4$ nanocomposite under UV irradiation (a) *S. aureus*, (b) *E. coli*.

References

1. Hrudey SE. Chlorination disinfection by-products, public health risk tradeoffs and me. Water Research. 2009;43(8):2057-92.
2. Huh AJ, Kwon YJ. "Nanoantibiotics": A new paradigm for treating infectious diseases using nanomaterials in the antibiotics resistant era. Journal of Controlled Release. 2011;156(2):128-45.
3. Wang X, Maeda K, Thomas A, Takanabe K, Xin G, Carlsson JM, et al. A metal-free polymeric photocatalyst for hydrogen production from water under visible light. Nature Materials. 2008;8(1):76-80.
4. Chegeni M, Mousavi Z, Soleymani M, Dehdashtian S. Removal of aspirin from aqueous solutions using graphitic carbon nitride nanosheet: Theoretical and experimental studies. Diamond and Related Materials. 2020;101:107621.
5. Low J, Yu J, Jaroniec M, Wageh S, Al-Ghamdi AA. Heterojunction Photocatalysts. Advanced Materials. 2017;29(20):1601694.
6. Mamba G, Mishra AK. Graphitic carbon nitride (g-C 3 N 4) nanocomposites: A new and exciting generation of visible light driven photocatalysts for environmental pollution remediation. Applied Catalysis B: Environmental. 2016;198:347-77.
7. Lam S-M, Sin J-C, Mohamed AR. A review on photocatalytic application of g-C3N4/semiconductor (CNS) nanocomposites towards the erasure of dyeing wastewater. Materials Science in Semiconductor Processing. 2016;47:62-84.
8. Huang D, Chen S, Zeng G, Gong X, Zhou C, Cheng M, et al. Artificial Z-scheme photocatalytic system: What have been done and where to go? Coordination Chemistry Reviews. 2019;385:44-80.
9. Yuan Y-P, Cao S-W, Liao Y-S, Yin L-S, Xue C. Red phosphor/g-C3N4 heterojunction with enhanced photocatalytic activities for solar fuels production. Applied Catalysis B: Environmental. 2013;140-141:164-8.
10. Chegeni M, Goudarzi F, Soleymani M. Synthesis, Characterization and Application of V 2 O 5 /S-Doped Graphitic Carbon Nitride Nanocomposite for Removing of Organic Pollutants. ChemistrySelect. 2019;4(46):13736-45.
11. Wang Z-T, Xu J-L, Zhou H, Zhang X. Facile synthesis of Zn(II)-doped g-C3N4 and their enhanced photocatalytic activity under visible light irradiation. Rare Metals. 2019;38(5):459-67.
12. Qin J, Huo J, Zhang P, Zeng J, Wang T, Zeng H. Improving the photocatalytic hydrogen production of Ag/g-C3N4 nanocomposites by dye-sensitization under visible light irradiation. Nanoscale. 2016;8(4):2249-59.
13. Hou Y, Ndamanisha JC, Guo L-p, Peng X-j, Bai J. Synthesis of ordered mesoporous carbon/cobalt oxide nanocomposite for determination of glutathione. Electrochimica Acta. 2009;54(26):6166-71.
14. Adhikari SP, Pant HR, Kim JH, Kim HJ, Park CH, Kim CS. One pot synthesis and characterization of Ag-ZnO/g-C3N4 photocatalyst with improved photoactivity and antibacterial properties. Colloids and Surfaces A: Physicochemical and Engineering Aspects. 2015;482:477-84.
15. Zhu M, Liu X, Tan L, Cui Z, Liang Y, Li Z, et al. Photo-responsive chitosan/Ag/MoS2 for rapid bacteria-killing. Journal of Hazardous Materials. 2020;383:121122.
16. Wang W, Zeng Z, Zeng G, Zhang C, Xiao R, Zhou C, et al. Sulfur doped carbon quantum dots loaded hollow tubular g-C3N4 as novel photocatalyst for destruction of Escherichia coli and tetracycline degradation under visible light. Chemical Engineering Journal. 2019;378:122132.
17. Ma S, Zhan S, Xia Y, Wang P, Hou Q, Zhou Q. Enhanced photocatalytic bactericidal performance and mechanism with novel Ag/ZnO/g-C3N4 composite under visible light. Catalysis Today. 2019;330:179-88.
18. Tian J, Liu Q, Asiri AM, Al-Youbi AO, Sun X. Ultrathin Graphitic Carbon Nitride Nanosheet: A Highly Efficient Fluorosensor for Rapid, Ultrasensitive Detection of Cu2+. Analytical Chemistry. 2013;85(11):5595-9.
19. Wayne, PA: Clinical and Laboratory Standards Institute; 2019.
20. Sobhani-Nasab A, Zahraei Z, Akbari M, Maddahfar M, Hosseinpour-Mashkani SM. Synthesis, characterization, and antibacterial activities of ZnLaFe 2 O 4 /NiTiO 3 nanocomposite. Journal of Molecular Structure. 2017;1139:430-5.
21. Deng L, Zhu M. Metal–nitrogen (Co-g-C3N4) doping of surface-modified single-walled carbon nanohorns for use as an oxygen reduction electrocatalyst. RSC Advances. 2016;6(31):25670-7.
22. Liu X, Li X, Shan Y, Yin Y, Liu C, Lin Z, et al. CuS nanoparticles anchored to g-C3N4 nanosheets for photothermal ablation of bacteria. RSC Advances. 2020;10(21):12183-91.
23. Zhou L, Wang L, Lei J, Liu Y, Zhang J. Fabrication of TiO2/Co-g-C3N4 heterojunction catalyst and its photocatalytic performance. Catalysis Communications. 2017;89:125-8.